Journal of Engineering Mathematics (2005) 52: 231–250
DOI 10.1007/s10665-004-2117-2

Some fundamental aspects of the continuumization problem in granular media

JOHN F. PETERS
U.S. Army Engineer Research and Development Center, Geotechnical and Structures Laboratory, Vicksburg, Mississippi 39180, U.S.A.

Received 18 September 2003; accepted in revised form 6 August 2004

Abstract. The central problem of devising mathematical models of granular materials is how to define a granular medium as a continuum. This paper outlines the elements of a theory that could be incorporated in discrete models such as the Discrete-Element Method, without recourse to a continuum description. It is shown that familiar concepts from continuum mechanics such as stress and strain can be defined for interacting discrete quantities. Established concepts for constitutive equations can likewise be applied to discrete quantities. The key problem is how to define the constitutive response in terms of truncated strain measures that are a practical necessity for analysis of large granular systems.

Key words: continuum mechanics, granular media, homogenization, stress

1. Introduction

Mathematicians and physicists who deal with granular media as a continuum must make a significant departure from traditional models. Attempts to classify granular states in terms of solid–fluid–gas phases have failed to produce a cogent theory of granular-media behavior [1], for while granular media ostensibly display all three states, for each case physical phenomena are observed that seem to lie outside of classical behavior. For most materials, there is a large separation between the micro-scale of atoms and molecules and macro-scale of measurements. This large separation of scales allows effective averaging on microscopic effects in time and space to create a continuum. For granular media, the fundamental particle is itself macroscopic, thus greatly reducing the importance of atomic-scale processes that are typically assumed to control properties. Thus, a clastic, such as sand, has more in common with the clutter flowing out of a closet than with the minerals of the rock from which it is derived. Although granular media might display the distinct states of solid, fluid, and gas, it is difficult to apply traditional continuum descriptions of these phases. The pressure dependence that controls dissipation in granular solids gives rise to profound mathematical difficulties in continuum formulations for stress analysis and wave propagation [2]. Flowing sand exhibits complex dynamic behavior not described by a Naiver–Stokes equation. Shear is not resisted by a simple viscosity, but by a combination of rate-independent processes including dilation, friction, and size separation. At variance to a gas, particle collisions are inelastic. In a gas-like state, granular media displays clustering, with formation of transient structures of particle chains. None of these features can be accommodated easily into a continuum-mechanics framework by simple readjustments of classical relationships of elasticity, plasticity, fluid mechanics, or gas dynamics. To understand particles as a "medium", it is necessary to build a theory from a particle-scale level in much the same manner that

thermodynamics was developed in the late 19th century. This paper draws attention to key aspects to modeling granular media as a continuum solid.

The discrete-element method (DEM) introduced by Cundal and Strack [3] provides a virtual laboratory for the study of granular physics by which it is possible to obtain measurements from simulations that would otherwise be impossible from physical experiments. In the absence of measurements made at the scale of supposed micro-mechanical mechanisms, the theories are essentially phenomenological. With the DEM, particle-scale theories become particularly compelling because they can be built on detailed measurement of deformations and forces at the particle scale. However, most theoretical efforts are couched in terms of continuum mechanics with the expressed goal of devising an equivalent continuum to represent the granular medium. An example is the procedure of Chang and Liao [4,5] where the discrete particle translation and rotation are "driven" by continuum motions. By application of the virtual work principle, continuum stress variables that are conjugate to the deformation variables can be obtained.

The motivation of continuumization granular for medium is reduction of the degrees of freedom that must be dealt with using a DEM approach. A DEM simulation is practically limited to a few million particles, which is equivalent to a handful of sand. Thus, to apply DEM to a prototype-scale problem typically requires use of oversized particles, which introduces scaling errors in the solution. By devising a constitutive equation of the equivalent medium, one can presumably employ a numerical solution to the partial differential equations that result from the continuumization process. However, at the particle scale, granular media do not behave as continua. In many problems, it is found that the kinematical freedom found in the DEM is a major part of the physics and that even a crude particle model can yield realistic results nearly impossible to obtain with a continuum-based approach [6,7]. In addition, the equivalent continuum response is not simple. As a minimum, the constitutive response of the equivalent continuum must contain higher-order terms to avoid mathematical ill-posedness inherent in frictional media. One might ask if the continuum description aids in making analysis of granular media tractable, or does it add a layer of abstraction that hinders progress.

The contribution of this paper to the growing discussion of granular continua is to propose an alternative tack by laying groundwork for analyses based on DEM. The question of continuumization is addressed by asking whether an equivalentcontinuum is in fact required. It is shown that the concepts of stress and strain can be conceived without the assumption of a continuum. Additionally, it is argued that plasticity effects caused by particle slip become more clear in a discrete medium because the oxymoronic notion of non-affine continuum motion is unnecessary. Thus, the principal tools needed to devise a mechanical theory of particulate media are provided. It is proposed that a fruitful avenue of research might be the behavior of coarsened DEM systems, including convergence properties of simulated granular media and averaged inter-particle contact laws that provide the sought-for equivalent behavior.

1.1. Notation

This paper employees two types of notation. When expressions contain subscripts, the standard indices notation of continuum mechanics is used. Tensor components are indicated by subscripts and repeated subscripts indicate summation. The identity tensor is signified as δ_{ij} and e_{ijk} is the permutation symbol. The superscript p signifies a quantity associated with a particle and superscript c signifies a quantity associated with a contact between two particles. Summation is not implied on repeated superscripts, but instead is explicitly indicated by

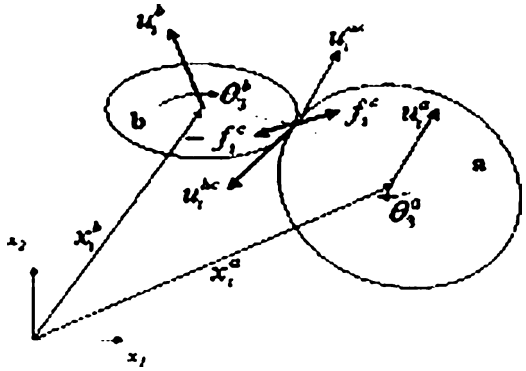

Figure 1. Kinematics of contact by a particle pair.

a summation symbol. The operation $|\cdot|$ is defined as $|\mathbf{f}| \equiv \sqrt{f_i f_i}$. Partial differentiation is denoted by $\nabla_i(\cdot) \equiv \partial(\cdot)/\partial x_i$.

In Section 4 a matrix notation is adopted to simplify the presentation of generalized stress and strain. The matrix operations are presented in the standard notation of linear algebra. The definitions of the matrices are given in Appendix A.

2. The discrete-element method

The discrete-element method provides a computational tool to study particulates without introducing the complications of a continuum theory. In DEM, the particles are treated as distinct interacting bodies. Interactions between particles are described by contact laws that define forces and moments created by relative motions of the particles. The motion of each particle that results from the net forces and moments are obtained by integrating Newton's laws. Thus, the particles are not treated as a medium. Rather, the medium behavior emerges from the interactions of the particles comprising the assemblage. The emergent behavior of the group is governed by relatively simple physical laws that obviate the need for complicated constitutive relationships [8].

The interaction (or contact) forces arise from relative motion between contacting particles. As shown in Figure 1, the motion of each individual particle is described by the velocity of the particle center and the rotation about the center. The branch vector between particle centers, $x_i^A - x_i^B$, is also the difference between the respective radii vectors that link the particle centers to the contact $r_i^A - r_i^B$. With this nomenclature, the relative motion at contact c between particles A and B is given by

$$\dot{\Delta}_i^c = \dot{u}_i^A - \dot{u}_i^B + e_{ijk}\left(r_j^A \dot{\theta}_k^A - r_j^B \dot{\theta}_k^B\right). \tag{1}$$

Under rigid-body motion there is no relative motion at any contacts. Rigid-body translation consists of $u_i^A = u_i^B$, with $\dot{\theta}_k^A = \dot{\theta}_k^B = 0$ for all particle pairs. Rigid-body rotation couples the particle rotation to the rotation of the particle assemblage. In this case, $\dot{\theta}_k^A = \dot{\theta}_k^B = \Omega_k$, where Ω_k is the rotation common to all points in the granular domain. For rigid body rotation therefore,

$$\dot{u}_i^A - \dot{u}_i^B = -e_{ijk}\left(r_j^A - r_j^B\right)\dot{\Omega}_k. \tag{2}$$

In three dimensions, there are three sets of rigid-body translations and three sets of rigid-body rotations. As will be discussed more precisely, the contact slip is equivalent to deformation in the system whereas the contact force is equivalent to stress.

3. Continuumization

The term *continuumization* refers to the process of representing a medium composed of individual discrete particles as a continuum having equivalent mechanical properties. This process is distinguished from more commonly used *homogenization* by recognition that a continuum implies a smoothness of motion with a preservation of connectedness not possessed by the granular media. Generally, the smoothness is imparted on the average motions of the particles, where the average is based on some representative elementary volume (REV). Many schemes have been proposed for finding an equivalent continuum. Chang and Liao [4], and more recently Tordesillas and Walsh [9] have tied particle motions to a smooth velocity using the virtual-work principle. Bardet and Vardoulakis [10] employed a similar method to elucidate the issue of non-symmetric stress tensor in Cosserat media. Bagi [11,12] considered the equilibrium of locally defined volumes obtained from Voronoi tessellation on particle centers. Kruyt [13] inspected graph properties of assemblages to define strain and stress variables.

In fact, there are two hierarchies of the continuum. The most basic concept of the continuum is statistically based in which the REV is chosen such that the fluctuation of the volumetric average is small. In this case, the REV acts as a smoother allowing discrete fields to be modeled as continuous. At the next level, deformation is viewed as affine mapping from some initial state to a final deformed state. Discontinuities can arise in finite number, which are dealt with through appropriate jump conditions. Ubiquitous discontinuities, such as slip, are sub-REV scale features and must be dealt with through abstractions such as internal variables that are effective mathematically but conceptually opaque.

This section deals with the first notion of the continuum. Averaging is performed on the governing equations imposing the momentum balance at the REV scale. The averaged equilibrium of the sampled volume is expressed in terms of stress which is derived from the averaging process. It is not assumed *a priori* that motions are affine. Rather, deformation rate is measured in terms of quantities that are thermodynamic conjugates to the stress. The sampled volume is said to be undergoing rigid-body motion if all relative motions among contacts are zero. The rigid-body motion have a null projection onto the space of deformations, which in effect, define those deformations. The projection of rigid-body motions onto the particle forces give rise to the equilibrium relationships for the sampled volume.

3.1. Properties of the average

For some function or operator f defined in the discrete medium contained within domain Ω, the average $\bar{f}$ of that quantity is defined at a point $x_i \in \Omega$ as

$$\bar{f}(x_i) = \int_{\Omega} \phi(x_i - x_i'; x_i) f(x_i') \mathrm{d}x_i'. \tag{3}$$

The present analysis considers an infinite domain to avoid influence of boundary terms. We specify that $\phi(x_i - x_i'; x_i) = \phi(x_i - x_i')$ where $\phi(x_i - x_i') = 0$ as $|x_i - x_i'| \to \infty$. Specifically, ϕ is assumed to have compact support, thus allowing a finite sampling volume $V \in \Omega$. With these restrictions it is necessary only that the integral of the weighting function over its range satisfy

$$\int_{\Omega} \phi(x_i - x_i') \mathrm{d}x_i' = \int_{V} \phi(x_i - x_i') \mathrm{d}x_i' = 1. \tag{4}$$

3.2. Weak equilibrium statement

The sampled space is composed of N^p particles, each with density ρ_s and volume V^p, accelerating at a_i^p. Interactions among particles occur at contacts through forces, f_i^c and moments m_i^c. For a typical particle, p, having N_c^p contacts, labeled $c \in N_c^p$, conservation of linear momentum requires

$$\sum_c^{N_c^p} f_i^c = V^p \rho^s a_i^p. \tag{5}$$

Each particle likewise rotates with acceleration ω_k^p, with rotational inertia I. For conservation of rotational momentum,

$$\sum_c^{N_c^p} \left(e_{ijk} r_j^c f_i^c + m_k^c \right) = \rho^s I \omega_k^p, \tag{6}$$

where r_j^c is the vector that connects the contact with the rotational center. Equations (5) and (6) must be satisfied for each particle within the domain. We wish to describe the equilibrium over the scale of the sampled volume as a weak form of the particle-scale conservation equations. That is, the weak form of the conservation statements requires that these statements are true when averaged via Equation (3). These averages are approximately

$$\sum_p^{N^p} \phi^p \sum_c^{N_c^p} f_i^c = \sum_p^{N^p} \phi^p V^p \rho^s a_i^p \tag{7}$$

and

$$\sum_p^{N^p} \phi^p \sum_c^{N_c^p} e_{ijk} r_j^c f_i^c = \sum_p^{N^p} \phi^p \rho^s I \omega_k^p. \tag{8}$$

3.3. Linear momentum

The process of averaging removes the spatial dependence on the particle quantities, such that the contact forces become statistical properties of the point for which the average is made. Accordingly, the summations on the left-hand side of in Equation (7) can be written as two summations over contacts within the sampling domain. The first summation is in terms of internal contacts which involve two particles. The second is for contacts at the domain boundary. For the internal contacts the contact force for respective particles A and B must satisfy $f_i^{Ac} = -f_i^{Bc} = f_i^c$, thus

$$\sum_c^{N^I} \left(\phi^A - \phi^B \right) f_i^c + \sum_c^{N^E} \phi^A f_i^{Ac} = \sum_p^{N^p} \phi^p V^p \rho^s a_i^p, \tag{9}$$

where the sum over the external contacts is zero owing to the prescribed properties of ϕ. Using the first term of the Taylor expansion for ϕ, the weighting can be applied at the contacts

$$\sum_c^{N^I} \nabla_j \phi^c \left(r_j^{Ac} - r_j^{Bc} \right) f_i^c = \sum_p^{N^p} \phi^p V^p \rho^s a_i^p, \tag{10}$$

where $\phi^c \equiv \phi(x_i - x_i^c)$, $x_i - x_i^c$ being the coordinate of the contact relative to the sampling point. The weighting function, ϕ^c is the only function of x_i in the summation.

3.4. Continuum stress

Within the domain the averaged linear momentum can be expressed as

$$\nabla_j \overline{\sigma}_{ij} = \overline{\rho a_i},$$

where

$$\overline{\sigma}_{ij} = \sum_c^{N^I} \phi^c \left(r_j^{Ac} - r_j^{Bc} \right) f_i^c. \tag{11}$$

In the event that mineral density ρ^s is the same for all grains and the acceleration is constant

$$\overline{\rho a_i} = \bar{\rho}\, \bar{a}_i,$$

where

$$\bar{\rho} = \rho^s \sum_p^{N^p} \phi^p V^p.$$

The summed quantity is the weighted integral over the solid volume and is the fraction of the sampled volume occupied by the solid phase. The density of that phase is ρ_s. The mean density $\bar{\rho}$ is the mass per *total* volume commonly referred to in soil mechanics as the total density.

3.5. Rotational momentum

Similar to the equation of linear momentum, the balance of rotational momentum can be written in the weak form to produce the counterpart of Equation (9)

$$\sum_c^{N^I} \nabla_l \phi^c \left(e_{ijk} \left(r_l^{Ac} r_j^{Ac} - r_l^{Bc} r_j^{Bc} \right) f_i^c + m_k^c r_l \right) + \sum_c^{N^E} \nabla_l \phi^c \left(e_{ijk} r_l^{Ac} r_j^{Ac} f_i^c + m_k^c r_l \right)$$
$$+ \sum_c^{N^I} \phi^c e_{ijk} \left(r_j^{Ac} - r_j^{Bc} \right) f_i^c + \sum_c^{N^E} \phi^c e_{ijk} r_j^{Ac} f_i^c = \sum_p^{N^p} \phi^p \rho^s I \omega_k^p. \tag{12}$$

Similar to Equation (11), the continuum expression can be written as

$$\nabla_l \overline{\mu}_{kl} + e_{ijk} \overline{\sigma}_{ij} = \overline{\rho^s I \omega_k^p},$$

where the $\overline{\mu}_{kl}$ is a coupled stress defined by

$$\overline{\mu}_{kl} = \sum_c^{N^I} \phi^c \left(e_{ijk} \left(r_l^{Ac} r_j^{Ac} - r_l^{Bc} r_j^{Bc} \right) f_i^c + m_k^c r_l \right). \tag{13}$$

Note that in the absence of contact couples, m_k^c, the coupled stress arises entirely from contact forces. In general the continuum stress $\overline{\sigma}_{ij}$ is not symmetric in the presence of a gradient in $\overline{\mu}_{kl}$ even if the contact moments are zero. The contribution of the contact forces to the asymmetry is a result of the resistance of the *finite* sampling volume to resist flexure-like deformation modes.

3.6. Work on unbalanced rotational forces

The presence of the moment gradient term leaves an unbalanced component in the moments created by the contact forces about a common center given in Equation (12). This moment does work against the rigid body rotation rate Ω_k as given by W_r

$$\dot{W}_r = \sum_c^{N^I} \phi^c e_{ijk} \left(r_j^{Ac} - r_j^{Bc} \right) f_i^c \Omega_k. \tag{14}$$

3.7. Power relationship

The deformation rate of the continuum is described by $\overline{D}_{ij}$, the symmetric part of the deformation tensor, Ω_k, the rotation of the sampling volume, and $\dot{\phi}_{kl}$ the rate of curvature. The deformation and curvature are linked to their respective particle quantities through a power balance whereby the work performed by the stress variables and their conjugate deformation variables is equal to that of contact forces and their conjugate contact motions,

$$\int_V \left(\overline{D}_{ij} \overline{\sigma}_{ij} + \Omega_k e_{ijk} \overline{\sigma}_{ij} + \dot{\phi}_{kl} \overline{\mu}_{kl} \right) \mathrm{d}V = \sum_c^{N_c} f_i^c \left[\Delta u_i^{AB} + e_{ijk} \left(r_j^A \omega_k^A - r_j^B \omega_k^B \right) \right] + W_r. \tag{15}$$

In view of Equations (11), (13), and (14)

$$\begin{aligned} &\sum_c^{N^I} \phi^c f_i^c \left(r_j^A - r_j^B \right) \left(\overline{D}_{ij} + e_{ijk} \Omega_k \right) + \sum_c^{N^I} \phi^c f_i^c e_{ijk} \left(r_l^A r_j^A - r_l^B r_j^B \right) \dot{\phi}_{kl} \\ &\quad = \sum_c^{N_c} f_i^c \left[\Delta u_i^{AB} + e_{ijk} \left(r_j^A \omega_k^A - r_j^B \omega_k^B \right) \right] + W_r. \end{aligned} \tag{16}$$

We immediately conclude that W_r cancels the work term associated with the motion $e_{ijk}\Omega_k$ on the left-hand side. The equality is satisfied for the particular case where

$$\dot{u}_i^{AB} + e_{ijk} \left(r_j^A \omega_k^A - r_j^B \omega_k^B \right) = \phi^c \left(\overline{D}_{ij} \left(r_j^A - r_j^B \right) + e_{ijk} \left(r_l^A r_j^A - r_l^B r_j^B \right) \dot{\phi}_{kl} \right). \tag{17}$$

By this procedure the particle centers are forced to follow the affine motion of the continuum, an obviously crude restriction if the constitutive relationships are to be built from the particle contact laws. The restriction in motion is the result of attempting to describe the many degrees of freedom of the finite sampling volume by the limited degrees of freedom represented by the deformation and curvature. This restriction can only be removed by including higher-order terms in the description of deformation. Another problem with Equation (17) is that the estimation of $\overline{D}_{ij}$ and $\dot{\phi}_{kl}$ from the motions of the particles requires an inversion of Equation (17). Both issues will be addressed from a more generalized conception of stress and strain.

4. Generalized stress and strain

Consider an assemblage of particles for which we wish to have measures of stress, σ, and strain, ϵ. The forces in the assemblage consist of contact forces between particles and external forces acting at the boundary of the sampling volume or as body forces. Whereas each particle has six degrees of freedom, the sampled volume has six N^p degrees of freedom, N_R of which are rigid-body motions that involve no relative movement between particles. The strain must

span a space of $M = N - N_R$ to completely capture all modes possible for the volume. Conjugate to this strain there are M generalized stress quantities. The task at hand is to define the operator that links the particle motion to the generalized strain and the forces to the generalized stress.

The translation and rotation of each particle is assigned to a generalized motion $\mathbf{u}$, which has a conjugate force and moment denoted as the generalized force $\mathbf{f}$ (See Appendix A). The force $\mathbf{f}$ is the vector of forces acting at the particle centers. These forces are the sum for each particle of the contact forces and body forces. As implied by the principle of virtual work, the conjugate pair $\mathbf{f}$ and $\dot{\mathbf{u}}$ should perform the same work as the conjugate σ and $\dot{\epsilon}$. Accordingly, the power balance is given by

$$\mathbf{f}^T \dot{\mathbf{u}} = \sigma^T \dot{\epsilon}. \tag{18}$$

Similarly, the contact forces, $\mathbf{f}_c$ and the conjugate contact motion, $\dot{\mathbf{\Delta}}_c$ should produce the same virtual work as σ and $\dot{\epsilon}$.

$$\mathbf{f}_c^T \dot{\mathbf{\Delta}}_c = \sigma^T \dot{\epsilon}. \tag{19}$$

This equivalence is the result of the fact that all mechanism of storing or dissipating energy are assumed to act at the contacts. (While this is a good approximation for the elastic processes, it is a fiction for the dissipative processes as is discussed in more detail in the section on internal variables.) The relationship between the particle motion and the contact motion of Equation (1) can be constructed in matrix form placing the relationships for each contact in the appropriate columns and rows of $\mathbf{M}$

$$\dot{\mathbf{\Delta}}_c = \mathbf{M}\dot{\mathbf{u}}. \tag{20}$$

By construction of $\mathbf{M}$, the relative motion between all contacts is zero for rigid-body motion. The rigid-body motions are known up to multiplicative constants. The direction vectors for the rigid body motions can be stored in the matrix $\mathbf{m}$, which constitute the null space of the operator $\mathbf{M}$,

$$\mathbf{M}\mathbf{m} = 0. \tag{21}$$

By the virtual work principle, the equilibrium relationship is given by

$$\mathbf{f}^T \mathbf{m} = \mathbf{0}. \tag{22}$$

The strain is a measure of relative movement among the particles, which is collectively perceived as the deformation of the assemblage. The strain rate is a linear transformation of the motion, $\dot{\mathbf{u}}$, given by Equation (23).

$$\dot{\epsilon} = \mathbf{B}\dot{\mathbf{u}}. \tag{23}$$

The null space of the operator $\mathbf{B}$ is given by the rigid-body motion, $\mathbf{m}$, as in Equation (21)[1]

$$\mathbf{B}\mathbf{m} = \mathbf{0}. \tag{24}$$

The relationship between $\mathbf{f}$ and σ immediately follows by substitution of Equation (23) in Equation (18).

$$\mathbf{f} = \mathbf{B}^T \sigma. \tag{25}$$

[1]The operator $\mathbf{B}$ must also satisfy the correct scale dependency. For example, in the particular case where $\mathbf{B}$ is a gradient operator, $\mathbf{B}\mathbf{x} = \mathbf{I}$, where $\mathbf{I}$ is the identity matrix.

Similarly, in view of Equations (18) and (19), the total force can be related to the contact force by

$$\mathbf{f} = \mathbf{M}^T \mathbf{f}_c. \tag{26}$$

Therefore, the distribution matrix, **M**, and the strain-displacement matrix, **B**, are equivalent in purpose. Further, the contact conjugate pairs $(\mathbf{f}_c, \dot{\mathbf{\Delta}}_c)$ and stress $(\sigma, \dot{\epsilon})$ should be directly related. To show this, note that the rank of **B** is $N - N_R$ by construction, thus there exists a right inverse

$$\mathbf{BAx} = \mathbf{x}. \tag{27}$$

It follows immediately that the stress is given in terms of the contact forces

$$\sigma = \mathbf{H}^T \mathbf{f}_c, \tag{28}$$

where

$$\mathbf{H} = \mathbf{MA}. \tag{29}$$

Substitute Equation (28) in the power balance, Equation (19), to get

$$\dot{\mathbf{\Delta}}_c = \mathbf{H}\dot{\epsilon}. \tag{30}$$

Thus, the stress and strain are equivalent to the contact force and displacement, respectively. The essential difference between the two conjugate pairs is that the contact pair $(\mathbf{f}_c, \dot{\mathbf{\Delta}}_c)$ depends on specifics of the arrangement of grains in the assemblage whereas the pair $(\sigma, \dot{\epsilon})$ can be viewed as measures for the complete ensemble, which take on standardized forms such as stretch, shear, flexure, and higher-order forms associated with continuum deformation.

4.1. Remark on examples of generalized strain

In Appendix B, examples of generalized strain measures are given for particle assemblages in two dimensions. It is noted that as more particles are added to the assemblage, additional modes appear in the definition of generalized strain. Thus, in a finite volume of particles, motions that describe deformation must satisfy the relationship $M = N_{DOF} N_p - N_R$, where M is the number of deformation modes for the assemblage, N_{DOF} is the number of degrees of freedom for each particle, N_P is the number of particles, and N_R is the number of rigid-body modes for the assemblage. For one-dimensional motion, $N_R = 1$; for two-dimensional motion $N_R = 3$; and for three-dimensional motion $N_R = 6$. The implication to any homogenization procedure is that it is necessary to either define deformation through higher-order terms, or to tie the "internal" higher-order modes to lower-order terms. The later choice requires an approximation that is part of the constitutive response of the assemblage.

4.2. Remark on finite-element stabilization

The construction of the **B** operator in the example computations of Appendix B is somewhat contrived because in finding the vectors orthogonal to **m** to populate **B**, choices were made to produce the traditional strain-displacement operators for finite elements. Clearly, other operators could be constructed from linear combinations of the rows of **B**. In each case, Equation (24) would be satisfied. Each definition of **B** carries with it a definition of stress and its conjugate strain. All definitions are equivalent in the sense that one definition can be derived from the other.

The procedure for obtaining **B** is similar to that for suppressing zero-energy modes in under-integrated finite elements described in [14]. In that case, the zero-energy modes are deformation modes that are not resisted by internal stresses. The finite elements are stabilized by determining a set of orthogonal modes to fully span the space. The forces associated with the added modes are determined from a simple proportionality between the force and deformation. The constant of proportionality is selected as a suitably large number to suppress the spurious modes and thereby stabilize the element.

4.3. Remark on constitutive response

If the generalized stress and strain concepts were to be employed to develop a continuum model, the issue of constitutive response for higher modes would become problematic. In contrast, building the constitutive response for the particle-scale level is straightforward in view of the duality between **B** and **M**. In the DEM approximation, all work is performed by contact forces giving the work balance in Equation (19). Assuming an elastic contact response

$$\dot{\mathbf{f}}_c = \mathbf{K}\dot{\mathbf{\Delta}}_c, \tag{31}$$

which immediately leads to (for small deformations),

$$\dot{\sigma} = \mathbf{D}\dot{\epsilon}, \tag{32}$$

where

$$\mathbf{D} = \mathbf{H}^T\mathbf{K}\mathbf{H}. \tag{33}$$

This result is similar to relationships by Tordesillas and Walsh [9], if account is taken of difference in notation.

5. Truncated strain measures

For most micro-mechanical formulations, the measure of strain is restricted to a few terms of a Taylor expansion centered within the REV. Alternatively, for application to coarsened particulate systems alluded to in the introduction, only a few representative particles are present. In either case, the strain measure is truncated leaving an approximation to the contact displacement. By casting Equation (17) in matrix form, the strain is projected to the contact quantities by

$$\dot{\bar{\mathbf{\Delta}}}_c = \overline{\mathbf{H}}\dot{\bar{\epsilon}}, \tag{34}$$

where the number of degrees of strain degrees of freedom are less than $N - N_R$. Consider the case where the contact displacements are known, either from a DEM simulation or experiment. The most representative strain is that which minimizes the square of residual

$$R^2 = \frac{1}{2}(\dot{\mathbf{\Delta}}_c - \overline{\mathbf{H}}\dot{\bar{\epsilon}})^T(\dot{\mathbf{\Delta}}_c - \overline{\mathbf{H}}\dot{\bar{\epsilon}}), \tag{35}$$

which leads to the least-squares approximation

$$\dot{\bar{\epsilon}} = (\overline{\mathbf{H}}^T\overline{\mathbf{H}})^{-1}\overline{\mathbf{H}}^T\dot{\mathbf{\Delta}}_c. \tag{36}$$

The strain can be expressed in terms of the particle motions by

$$\dot{\bar{\epsilon}} = (\overline{\mathbf{H}}^T\overline{\mathbf{H}})^{-1}\overline{\mathbf{H}}^T\mathbf{M}\dot{\mathbf{u}}. \tag{37}$$

The stress is given by

$$\bar{\sigma} = \overline{\mathbf{H}}^T \mathbf{f}_c. \tag{38}$$

Note that an implication of Equation (38) is that $\overline{\mathbf{H}}$ can be obtained by converting Equations (11) and (13) into matrix form. Thus, given the averaged stress in terms of particle-scale quantities, the correct definition of the conjugate strain rate, in terms of particle-scale quantities, follows immediately via Equation (36).

5.1. Elastic constitutive response

The form of the relationships for stress and strain are analogous to Equations (23) and (28) and lead to a constitutive relationship that is similar to Equation (32), $\bar{\sigma} = \bar{\mathbf{D}}\bar{\epsilon}$. It is well known that the resulting stress–strain response is too stiff compared to that measured for the assemblage [4]. The stiff response is the result of the constraint imposed on the displacements and it is expected that as more terms are added to the strain, the response will match the assemblage response better. The situation can be understood by considering Equation (33) in a partitioned form.

$$\begin{bmatrix} \mathbf{D}_{uu} & \mathbf{D}_{ul} \\ \mathbf{D}_{ul}^T & \mathbf{D}_{ll} \end{bmatrix} \begin{Bmatrix} \dot{\bar{\epsilon}} \\ \dot{\epsilon}' \end{Bmatrix} = \begin{Bmatrix} \dot{\bar{\sigma}} \\ \dot{\sigma}' \end{Bmatrix}. \tag{39}$$

The barred quantities correspond to those strain terms included in the truncated strain. The primed quantities are the additional terms required to span the space. Note especially that in general $\bar{\mathbf{D}} \neq \mathbf{D}_{uu}$. Possible approaches to account for the truncated terms are considered as the following three cases:

5.1.1. *Case 1:* $\dot{\epsilon}' = 0$

This case corresponds to projecting the truncated strain measure (*e.g.* Equation (17)) such that

$$\mathbf{D}_{uu}\dot{\bar{\epsilon}} = \dot{\bar{\sigma}}, \tag{40}$$

with the internal stress terms given as

$$\dot{\sigma}' = \mathbf{D}_{ul}^T \dot{\bar{\epsilon}}. \tag{41}$$

This case corresponds physically to an interlocked structure that does not allow significant inter-grain motion.

5.1.2. *Case 2:* $\dot{\sigma}' = 0$

In this case, the internal stress terms are absent and the higher-order modes of deformation are not resisted. The constitutive equation for this case would be

$$(\mathbf{D}_{uu} - \mathbf{D}_{ul}\mathbf{D}_{ll}^{-1}\mathbf{D}_{ul}^T)\dot{\bar{\epsilon}} = \dot{\bar{\sigma}}, \tag{42}$$

with

$$\dot{\epsilon}' = -\mathbf{D}_{ll}^{-1}\mathbf{D}_{ul}^T \dot{\bar{\epsilon}}. \tag{43}$$

The higher-order strains become linear functions of the truncated strains. This case can be readily shown to result from minimizing $\dot{\epsilon}^T \mathbf{D} \dot{\epsilon}$ with respect to $\dot{\epsilon}'$, which corresponds physically to a relaxed structure where granular motion is essentially not resisted.

5.1.3. *Case 3:* $\dot{\epsilon}' \neq 0$ *and* $\dot{\sigma}' \neq 0$
The general stiffness relationship is

$$(\mathbf{D}_{uu} - \mathbf{D}_{ul}\mathbf{D}_{ll}^{-1}\mathbf{D}_{ul}^{T})\dot{\bar{\epsilon}} = \dot{\bar{\sigma}} - \mathbf{D}_{ul}\mathbf{D}_{ll}^{-1}\dot{\sigma}', \tag{44}$$

with

$$\dot{\epsilon}' = \mathbf{D}_{ll}^{-1}(\dot{\sigma}' - \mathbf{D}_{ul}^{T}\dot{\bar{\epsilon}}). \tag{45}$$

To close the system of equations a relationship is required to define either $\dot{\sigma}'$ or $\dot{\epsilon}'$. It is seen that in general, the *Case 2*, where $\dot{\epsilon}'$ is a linear function of $\dot{\bar{\epsilon}}$, corresponds to the fully relaxed case, where $\dot{\sigma}' = 0$, whereas *Case 1*, where $\dot{\sigma}'$ is a linear function of $\dot{\bar{\sigma}}$, corresponds to the fully locked where $\dot{\epsilon}' = 0$. The evolution of the structure from one case to another is a dissipative process implying an additional constitutive equation of the type

$$\dot{\sigma}' = \mathbf{A}\dot{\bar{\epsilon}} - \alpha\sigma'.$$

6. Internal variables

In the preceding discussion, a process is proposed in which the granular structure transitions from a completely locked assemblage, which is entirely elastic, to a completely relaxed structure where particle motions are unrestricted. For elastic deformation the topology of the assemblage remains constant such that contacts are not broken nor are new contacts made. Thus, the assemblage can be viewed as an elastic system in which the state of the system is determined entirely by the strain. From the standpoint of solid mechanics, the particulate medium could be homogenized into an elastic solid described by a higher-order strain theory. In the more general case of evolving structure, the state of the system is no longer described completely by the strain because the processes of contact creation and breakage are irreversible, a fact that must be considered for describing any homogenized continuum description of the medium. In continuum mechanics, such non-affine motions are addressed through internal variables, which account for the irreversible mechanisms within the medium. Internal variable theory provides the formal framework for irreversibility such that it is possible to devise models for materials undergoing irreversible changes in internal structure without violating the principles of thermodynamics (*e.g.* [15]). However, the theory does not describe specifically what physical process the internal variables represent, leaving their meaning in phenomenological models somewhat murky. Some authors have related internal variables in plasticity models to slips or diffusion of dislocations in some limited crystalline systems, but models that are more comprehensive generally express their meaning with vague reference to internal processes. More notable is the effort to relate the internal variables to those additional motions that are not captured by the strain. However, as emphasized by Valanis and Lee [16], such deformation must include non-affine motion to qualify as an internal variable. It is implied that such motion is accompanied by changes in the material topology, a process more easily visualized at the particle scale.

A theory that is built up from a particle-scale model has the advantage that the meaning of the internal variable is clear in the sense that internal variables can be computed from particle-scale measurement, whether based on experiments or simulation. The most obvious notion of an internal variable is that of contact slip. Generally, a Coulomb friction law is applied at the contact such that the contact motion includes a slip giving a contact law

$$f_i^c = K_{ij}^c(\Delta_j^c - \delta_j^c), \tag{46}$$

where δ_i^c is the component of contact motion that represents slip. The evolution law for the slip is

$$\dot{\delta}_i^c = \begin{cases} 0 & \text{for } |\tau_i^c| < \mu\sigma^c, \\ \dot{\Delta}_i^c & \text{for } |\tau_i^c| = \mu\sigma^c, \end{cases} \tag{47}$$

where $\sigma^c = f_i^c n_i^c$, $\tau_i^c = f_i^c - f_j^c n_j^c n_i^c$, and μ is the Coulomb friction coefficient. The combined result of Equations (46) and (47) ensure that $|\tau_i^c|$ can never exceed $\mu\sigma^c$.

In reality, slip is not this simple. In a time step, a contact can be created or lost, which at the macro level has the effect of slip. Consider a finite time increment $\Delta t = t_1 - t_o$, during which a particle makes contact and gives rise to a contact force f_i^c, beginning at t_c. The total motion of the particles making the contact is $\dot{\Delta}_i^c \Delta t$. Of this total motion, only the part $\dot{\Delta}_i^c (t_c - t_o)$ actually contributes to the contact force. That is, the average rate is

$$\begin{aligned} \dot{f}_i^c &= K_{ij}^c \left(\dot{\Delta}_j^c \Delta t - \dot{\Delta}_j^c (t_c - t_o) \right) / \Delta t \\ &= K_{ij}^c \left(\dot{\Delta}_j^c - \dot{\delta}_j^c \right) \end{aligned} \tag{48}$$

A simular argument can be made for contacts lost over a time step.

Within the REV many contacts are formed and lost over a time step. These contacts can be binned based on the contact orientation. Each orientation is represented by six rows of matrix **H** (see Appendix A). Thus, $\dot{\Delta}_i^c = H_{ik}^c \dot{\epsilon}_k$. The slip component can similarly be expressed in terms of a macroscopic variable by $\dot{\delta}_i^c = H_{ij}^c q_j$. The portion of the stress, denoted Q_i^c that arises from a particular contact direction is $Q_i^c = H_{ki}^c f_k^c$. The macroscopic law is

$$\dot{Q}_i^c = H_{ki}^c H_{jl}^c K_{kj}^c \left(\dot{\epsilon}_l - \dot{q}_l^c \right), \tag{49}$$

with

$$\sigma_i = \sum_c Q_i^c. \tag{50}$$

A key observation from Equation (49) is that q_j^c is a function of the contact direction implying that no single of q_j^c can describe slips for all contact directions. Thus, the complete constitutive law involves multiple internal variables.

Equations (49) and (50) are equivalent to those produced by an internal variable law based on a Helmholtz free energy $\psi(\epsilon, \mathbf{q}_c) = \sum_c \psi^c(\epsilon, \mathbf{q}^c)$ where

$$\psi^c = D_{ij}^c (\epsilon_i - q_i^c)(\epsilon_j - q_j^c), \tag{51}$$

with

$$\sigma_i = \frac{\partial \psi}{\partial \epsilon_i}, \tag{52}$$

and

$$Q_i^c = -\frac{\partial \psi}{\partial q_i^c}. \tag{53}$$

The evolution of $\mathbf{q}^c$ is an object for research. In any case, the evolution law must satisfy the second law of thermodynamics which implies

$$-\dot{q}_i^c \frac{\partial \psi}{\partial q_i^c} \geq 0. \tag{54}$$

For tangential slip, Equation (47) guarantees that inequality (54) is satisfied. For normal motion at contacts, the situation is more complicated. In DEM simulations, it is necessary to apply some sort of damping to the normal contact law. Physically, a hysteretic law is reasonable, because it maintains rate-independence of the dissipation, although in practice some viscous damping is also needed. These mechanism of energy dissipation obey the inequality (54) as well. The challenge is to make particle-scale measurements that clearly relate these mechanisms of particle interactions to the internal variables. The work of Zhang and Raueszahn [17] is notable in this regard for granular flows.

It should be recognized that $\mathbf{H}^c$ evolves in response to both elastic and inelastic changes to the particulate structure. Its evolution must conform with the second law given by the inequality

$$-\frac{\partial \psi}{\partial \mathbf{H}^c}\dot{\mathbf{H}}^c \geq 0. \tag{55}$$

That is, changes in $\mathbf{H}^c$ due to changes in internal structure cannot increase the free energy.

7. Conclusions

This paper began with a demonstration that continuum equations for the conservation of linear and rotational momentum can obtained from spatial averaging of the particle-scale momentum balance equations to produce the equations of a Cosserat medium. Two points emerged from this effort. First, the stress quantities need not be defined as averages of any local stress but arise naturally as result of spatial averaging of the equilibrium equations. Second, simple projections of conjugate deformation measures cannot be used in micro-scale constitutive relationships because such average motions are overly restricted. It is later shown that either higher-order deformation measures must be introduced, or the average motion as part of the constitutive relationship must drive particle-scale motions. In arriving at that conclusion, it is first shown that the concepts of stress and strain can be generalized to encompass the discrete quantities at the particle scale without recourse to the continuum concept. These generalized stresses and strains are shown to be equivalent to motions and forces at contacts, which allows deriving macro-scale constitutive equations from particle-scale relationship. The deformation conjugates to the averaged stress tensors are observed to be truncated forms of the generalized stress vector. The commonly used least-squares procedure is shown to provide strain measures that are conjugate to the averaged stress measures. Significantly, it is shown that the general concepts associated with constitutive theory for continua can be employed without the specific use of the continuum concept. It is concluded that a coarsened DEM could accordingly be developed.

Appendix A. Matrix nomenclature

The matrix nomenclature is introduced to make the general structure of the theory more clear. The displacement of each particle center is described by six degrees of freedom, $(u_x, u_y, u_z, \theta_x, \theta_y, \theta_z)$, which are arranged in $\mathbf{u}$ matrix as follows:

$$\begin{aligned}\mathbf{u}^T = [&(u_x^1, u_x^2, \ldots, u_x^{N_p}), (u_y^1, u_y^2, \ldots, u_y^{N_p}), (u_z^1, u_z^2, \ldots, u_z^{N_p}),\\ &(\theta_x^1, \theta_x^2, \ldots, \theta_x^{N^P})(\theta_y^1, \theta_y^2, \ldots, \theta_y^{N^P})(\theta_z^1, \theta_z^2, \ldots, \theta_z^{N^P})]\end{aligned} \tag{A.1}$$

The conjugate force vector $\mathbf{f}$ is arranged as $(f_x, f_y, f_z, m_x, m_y, m_z)$, so that

$$\begin{aligned}\mathbf{f}^T = &[(f_x^1, f_x^2, \ldots, f_x^{N_p}), (f_y^1, f_y^2, \ldots, f_y^{N_p}), (f_z^1, f_z^2, \ldots, f_z^{N_p}),\\ &(m_x^1, m_x^2, \ldots, m_x^{N^P})(m_y^1, m_y^2, \ldots, m_y^{N^P})(m_z^1, m_z^2, \ldots, m_z^{N^P})]\end{aligned} \tag{A.2}$$

Therefore, the quantity $\mathbf{f}^T\mathbf{u}$ is the sum of the work for the particle assemblage.

The stress and strain are simply

$$\sigma^T = [\sigma_1, \sigma_2, \ldots, \sigma_N] \tag{A.3}$$

and

$$\epsilon^T = [\epsilon_1, \epsilon_2, \ldots, \epsilon_N]. \tag{A.4}$$

The contact quantities consist of $(\Delta_x, \Delta_y, \Delta_z, \Theta_x, \Theta_y, \Theta_z)$, where Θ_i is the difference in rotation between contacting particles. These are grouped in $\Delta_\mathbf{c}$ in accordance with the contact number. The forces conjugate to the contact degree of freedom are $(f_x^c, f_y^c, f_z^c, m_x^c, m_y^c, m_z^c)$ and are likewise arranged in accordance with the contact number. The matrix $\mathbf{M}$ is constructed using the relationships between particle motion and contact motion,

$$\Delta_i^c = u_i^A - u_i^B + e_{ijk}(r_j^A\dot{\theta}_k^A - r_j^B\dot{\theta}_k^B). \tag{A.5}$$

and

$$\Theta_i = \theta^A - \theta^B. \tag{A.6}$$

The rows of $\mathbf{M}$ correspond to the components of $\mathbf{\Delta}_c$ and $\mathbf{f_c}$, whereas the columns correspond to the ordering of $\mathbf{u}$ and $\mathbf{f}$. For example, for $\mathbf{\Delta}_c = \mathbf{Mu}$,

$$\begin{Bmatrix} \vdots \\ \Delta_x \\ \Delta_y \\ \Delta_z \\ \Theta_x \\ \Theta_y \\ \Theta_z \\ \vdots \end{Bmatrix} = \begin{bmatrix} \ldots & 1 & 0 & 0 & \ldots & -1 & 0 & 0 & \ldots & 0 & -r_z & r_y & \ldots & 0 & r_y & -r_y & \ldots \\ \ldots & 0 & 1 & 0 & \ldots & 0 & -1 & 0 & \ldots & r_z & 0 & -r_x & \ldots & -r_z & 0 & r_x & \ldots \\ \ldots & 0 & 0 & 1 & \ldots & 0 & 0 & -1 & \ldots & -r_y & r_x & 0 & \ldots & r_y & -r_x & 0 & \ldots \\ \ldots & 0 & 0 & 0 & \ldots & 0 & 0 & 0 & \ldots & 1 & 0 & 0 & \ldots & -1 & 0 & 0 & \ldots \\ \ldots & 0 & 0 & 0 & \ldots & 0 & 0 & 0 & \ldots & 0 & 1 & 0 & \ldots & 0 & -1 & 0 & \ldots \\ \ldots & 0 & 0 & 0 & \ldots & 0 & 0 & 0 & \ldots & 0 & 0 & 1 & \ldots & 0 & 0 & -1 & \ldots \end{bmatrix}. \tag{A.7}$$

The $\mathbf{H}$ matrix is arranged similarly except that the columns correspond to ordering of the strain components. The rigid body motion is specified up to an arbitrary constant and is given by

$$\begin{aligned}&\underline{\text{Translation}},\ \theta_1 = \theta_2 = \theta_3 = 0\\ &x = 1\\ &y = 1\\ &z = 1\\ &\underline{\text{Rotation}},\\ &u_i = e_{ij1}x_j, \quad \theta_1 = 1, \quad \theta_2 = \theta_3 = 0\\ &u_i = e_{ij2}x_j, \quad \theta_1 = 0, \quad \theta_2 = 1, \quad \theta_3 = 0\\ &u_i = e_{ij3}x_j, \quad \theta_1 = 0, \quad \theta_2 = 0, \quad \theta_3 = 1\end{aligned} \tag{A.8}$$

The **m** matrix is constructed such that its six rows constitute these rigid-body motions and the columns correspond to the ordering used for **u** and **f**.

$$\mathbf{m}=\begin{bmatrix} 1 & 0 & 0\,0\,0\,0 \\ 0 & 1 & 0\,0\,0\,0 \\ 0 & 0 & 1\,0\,0\,0 \\ 0 & -\mathbf{z} & \mathbf{y}\,1\,0\,0 \\ -\mathbf{z} & 0 & \mathbf{x}\,0\,1\,0 \\ \mathbf{y} & -\mathbf{x} & 0\,0\,0\,1 \end{bmatrix} \tag{A.9}$$

where **I** is the identity matrix and

$$\mathbf{1}=[1,1,1,\ldots,1], \tag{A.10}$$

$$\mathbf{0}=[0,0,0,\ldots,0], \tag{A.11}$$

$$\mathbf{x}=[x_1,x_2,x_3,\ldots,x_{N^p}], \tag{A.12}$$

$$\mathbf{y}=[y_1,y_2,y_3,\ldots,y_{N^p}], \tag{A.13}$$

$$\mathbf{z}=[z_1,z_2,z_3,\ldots,z_{N^p}]. \tag{A.14}$$

Appendix B. Example of constructing B

B.1. General case

Construction of the **B** matrix amounts to filling out the **m** matrix given in Equation A.9 with orthogonal rows. Noting the structure of **m**, the process is facilitated by constructing **B** from sub-matrices as shown in Figure B1.

The properties of the sub-matrices follow from the orthogonality requirement, specifically, $\mathbf{L}_i \cdot \mathbf{1} = \mathbf{N}_i \cdot \mathbf{1} = 0$, and $\mathbf{L}_i \cdot \mathbf{x_j} = \mathbf{N}_i \cdot \mathbf{x_j} = 0$ for $i \neq j$. The sub-matrices are scaled such that $\mathbf{L}_i \cdot \mathbf{x_i} = \mathbf{N}_i \cdot \mathbf{x_i} = 1$ The sub-matrices $\mathbf{J}_i$ must satisfy the simpler orthogonality relationship $\mathbf{J}_i \cdot \mathbf{1} = 0$. The sub-matrices $\mathbf{M}_i$ are computed to satisfy the relationship

$$\mathbf{N}_x \cdot \mathbf{x}_x + \mathbf{N}_y \cdot \mathbf{x_y} + \mathbf{M}_z \cdot \mathbf{1} = 0,$$

for all permutations of x, y, and z.

The construction of **B** are given for specific cases in the sections that follow.

B.2. Three-particle assemblage

Consider an example of a three-particle assemblage moving within a plane. The rigid-body motions using the format of Equation (A.9), are

$$\mathbf{m}=\begin{bmatrix} 1 & 1 & 1 & 0 & 0 & 0 & 0\,0\,0 \\ 0 & 0 & 0 & 1 & 1 & 1 & 0\,0\,0 \\ y_1 & y_2 & y_2 & -x_1 & -x_2 & -x_3 & 1\,1\,1 \end{bmatrix}. \tag{B.1}$$

The first row represent uniform translation in the x-direction, the second represents uniform translation in the y-direction, and the third is rigid-body motion in which the particle rotations are equal to the rigid-body rotation of the assemblage about the origin.

It is useful to consider the reduced form shown in Figure B2 that corresponds to two-dimensional motion in the x-y plane. The columns corresponding to translation in the z-direction and rotations about the x and y axes are removed. Accordingly, rows corresponding to gradients of those degrees of freedom are removed.

$$\begin{Bmatrix} \mathbf{m} \\ \text{- -} \\ \mathbf{B} \end{Bmatrix} = \begin{bmatrix} \mathbf{1} & \mathbf{0} & \mathbf{0} & \mathbf{0} & \mathbf{0} & \mathbf{0} \\ \mathbf{0} & \mathbf{1} & \mathbf{0} & \mathbf{0} & \mathbf{0} & \mathbf{0} \\ \mathbf{0} & \mathbf{0} & \mathbf{1} & \mathbf{0} & \mathbf{0} & \mathbf{0} \\ \mathbf{0} & -\mathbf{z} & \mathbf{y} & \mathbf{1} & \mathbf{0} & \mathbf{0} \\ -\mathbf{z} & \mathbf{0} & \mathbf{x} & \mathbf{0} & \mathbf{1} & \mathbf{0} \\ \mathbf{y} & -\mathbf{x} & \mathbf{0} & \mathbf{0} & \mathbf{0} & \mathbf{1} \\ \text{- -} & \text{- -} & \text{- -} & \text{- -} & \text{- -} & \text{- -} \\ \mathbf{L}_x & \mathbf{0} & \mathbf{0} & \mathbf{0} & \mathbf{0} & \mathbf{0} \\ \mathbf{0} & \mathbf{L}_y & \mathbf{0} & \mathbf{0} & \mathbf{0} & \mathbf{0} \\ \mathbf{0} & \mathbf{0} & \mathbf{L}_z & \mathbf{0} & \mathbf{0} & \mathbf{0} \\ \mathbf{0} & \mathbf{0} & \mathbf{0} & \mathbf{J}_x & \mathbf{0} & \mathbf{0} \\ \mathbf{0} & \mathbf{0} & \mathbf{0} & \mathbf{0} & \mathbf{J}_y & \mathbf{0} \\ \mathbf{0} & \mathbf{0} & \mathbf{0} & \mathbf{0} & \mathbf{0} & \mathbf{J}_z \\ \mathbf{N}_y & \mathbf{N}_x & 0 & 0 & 0 & 0 \\ \mathbf{0} & \mathbf{N}_z & \mathbf{N}_y & \mathbf{0} & \mathbf{0} & \mathbf{0} \\ \mathbf{N}_z & \mathbf{0} & \mathbf{N}_x & \mathbf{0} & \mathbf{0} & \mathbf{0} \\ \mathbf{0} & \mathbf{0} & \mathbf{0} & \mathbf{J}_y & \mathbf{0} & \mathbf{0} \\ \mathbf{0} & \mathbf{0} & \mathbf{0} & \mathbf{J}_z & \mathbf{0} & \mathbf{0} \\ \mathbf{0} & \mathbf{0} & \mathbf{0} & \mathbf{0} & \mathbf{J}_x & \mathbf{0} \\ \mathbf{0} & \mathbf{0} & \mathbf{0} & \mathbf{0} & \mathbf{J}_z & \mathbf{0} \\ \mathbf{0} & \mathbf{0} & \mathbf{0} & \mathbf{0} & \mathbf{0} & \mathbf{J}_y \\ \mathbf{0} & \mathbf{0} & \mathbf{0} & \mathbf{0} & \mathbf{0} & \mathbf{J}_x \\ \mathbf{N}_y & -\mathbf{N}_x & \mathbf{0} & \mathbf{0} & \mathbf{0} & \mathbf{M}_z \\ \mathbf{0} & -\mathbf{N}_z & \mathbf{N}_y & \mathbf{M}_x & \mathbf{0} & \mathbf{0} \\ \mathbf{N}_z & \mathbf{0} & -\mathbf{N}_x & \mathbf{0} & \mathbf{M}_y & \mathbf{0} \end{bmatrix}$$

Figure B1. General form of **B**.

$$\begin{Bmatrix} \mathbf{m} \\ \text{- - -} \\ \mathbf{B} \end{Bmatrix} = \begin{bmatrix} \mathbf{1} & \mathbf{0} & \mathbf{0} \\ \mathbf{0} & \mathbf{1} & \mathbf{0} \\ \mathbf{y} & -\mathbf{x} & \mathbf{1} \\ \text{- - -} & \text{- - -} & \text{- - -} \\ \mathbf{L}_x & \mathbf{0} & \mathbf{0} \\ \mathbf{0} & \mathbf{L}_y & \mathbf{0} \\ \mathbf{N}_y & \mathbf{N}_x & \mathbf{0} \\ \mathbf{0} & \mathbf{0} & \mathbf{J}_y \\ \mathbf{0} & \mathbf{0} & \mathbf{J}_x \\ \mathbf{N}_y & -\mathbf{N}_x & \mathbf{M}_z \end{bmatrix}$$

Figure B2. Form of **B** for deformation in x–y plane.

The number of rows of the **B** matrix is given by $M = N_{DOF}N_p - N_R$, for two-dimensional motion, $N_{DOF} = 3$ and $N_R = 3$. Thus, $M = 6$ implying that each sub-matrix contains one row. Thus we set $\mathbf{L}_i = \mathbf{N}_i = \mathbf{J}_i$ for all i. The $\mathbf{L}_x$ sub-matrix is orthogonal to $(1, 1, 1)$ and (y_1, y_2, y_3) and can be computed from the cross product between these two vectors. Denoting the cross product as $\mathbf{L}_x^*$, then $\mathbf{L}_x = a\mathbf{L}_x^*$, where $a = 1/(\mathbf{L}_x^* \cdot \mathbf{x})$. The sub-matrix $\mathbf{L}_y$ can be found in a similar manner. It is easily verified by direct substitution that $\mathbf{L}_x^* \cdot \mathbf{x} = \mathbf{L}_y^* \cdot \mathbf{y}$.

$$\mathbf{B} = a \begin{bmatrix} y_{32} & y_{13} & y_{21} & 0 & 0 & 0 & 0 & 0 & 0 \\ 0 & 0 & 0 & x_{23} & x_{31} & x_{12} & 0 & 0 & 0 \\ x_{23} & x_{31} & x_{12} & y_{32} & y_{13} & y_{21} & 0 & 0 & 0 \\ 0 & 0 & 0 & 0 & 0 & 0 & y_{31} & y_{13} & y_{21} \\ 0 & 0 & 0 & 0 & 0 & 0 & x_{23} & x_{31} & x_{12} \\ x_{23} & x_{31} & x_{12} & y_{23} & y_{31} & y_{12} & M_\theta & M_\theta & M_\theta \end{bmatrix}, \tag{B.2}$$

where $y_{IJ} = y_I - y_J$, $x_{IJ} = x_I - x_J$, and The sub-matrix $\mathbf{M}_\theta$ are equal and are given by

$$M_\theta = 2(y_{32}x_1 + y_{13}x_2 + y_{21}x_3).$$

The matrix corresponds to the strain-displacement matrix for a constant strain triangular finite element with terms included for the Cosserat rotations. The factor a is equal to twice the area defined by the line segments connecting the three particle centers. The first two rows of **B** correspond to the gradient of velocity in the x- and y-directions, respectively. The third row represents shear. The fourth and fifth rows correspond to the gradients of rotations in the x- and y-directions, respectively. The sixth row corresponds to the difference between the rigid body rotation of the assemblage and the average particle rotation.

B.3. Four-particle assemblage

In the case of a four-particle assemblage with two-dimensional motion, the strain operator would again contain terms for the strains, Cosserat curvatures, and rotations. In this case $N_p = 4$ requiring that $M = 9$. Thus, three rows must be added. However, the matrix shown in Figure B2 remains applicable implying that the sub-matrices contain multiple rows. For the special case where the particle rotation is not included, the matrix shown in Figure B2 is reduced to three rows with five independent vectors required. Thus, of the three vectors required, only one is associated with the rotations.

Consider the case of $\mathbf{L}_x$. The possible vectors that meet the orthogonality conditions can be obtained from a cross product in R^4. For any vector, $\mathbf{l}$ in R^4 that is not parallel with either $\mathbf{1}$ or $\mathbf{y}$, $\mathbf{L}_x$ is given by

$$\mathbf{L}_x = \begin{Bmatrix} l_2(y_4 - y_3) + l_3(y_2 - y_4) + l_4(y_3 - y_2) \\ l_1(y_3 - y_4) + l_3(y_4 - y_1) + l_4(y_1 - y_3) \\ l_1(y_4 - y_2) + l_2(y_1 - y_4) + l_4(y_2 - y_1) \\ l_1(y_2 - y_3) + l_2(y_3 - y_1) + l_3(y_1 - y_2) \end{Bmatrix}. \tag{B.3}$$

For any valid assemblage, $\mathbf{l} = \mathbf{x}$ is can be used to generate $\mathbf{L}_x$. For the particular case of a square array of particles with $\mathbf{x} = (-1, 1, 1, -1)$ and $\mathbf{y} = (-1, -1, 1, 1)$, $\mathbf{L}_x$ is found to be

$$\mathbf{L}_x = \begin{bmatrix} -1 & 1 & 1 & -1 \\ -4 & 4 & -4 & 4 \end{bmatrix}. \tag{B.4}$$

The first row corresponds to a uniform expansion of the particles in the x-direction. The second row represents a flexure mode, commonly referred to as an hour-glass mode in the finite-elements literature. The case for $\mathbf{L}_y$ is similar. The additional mode associated with rotation can be similarly computed by taking the cross product in R^4 for the set $\mathbf{1}$, $\mathbf{L}_x$, and $\mathbf{L}_y$. The result is a pattern corresponding to the flexure mode.

B.4. Nearest-neighbor configuration

The nearest-neighbor configuration consists of a central particle surrounded by three particles such that $\mathbf{x} = (0, -1, 1, 0)$ and $\mathbf{y} = (\sqrt{3}/2, 0, 0, \sqrt{3})$. This arrangement is similar to that used for the micro-mechanical modeling by Tordesillas and Walsh [9]. The relationships for this four particle assemblage is the same as the preceeding example. The sub-matrix $\mathbf{L}_x$ obtained in this case illustrates the difference made by the coordinate location of the fourth particle.

$$\mathbf{L}_x = \begin{bmatrix} 0 & -1 & 1 & 0 \\ -2\sqrt{3} & \dfrac{\sqrt{3}}{2} & \dfrac{\sqrt{3}}{2} & \dfrac{\sqrt{3}}{2} \end{bmatrix}. \tag{B.5}$$

As for the preceding example, the first row corresponds to a uniform stretch in the x-direction. However, the second row corresponds to a motion of the central particle relative to the three surrounding particle, which is quite unlike the flexure modes of the four-corner configuration. It is significant that these two modes are orthogonal; the deformation $\overline{D}_{ij}$ of Equation (17) provides no information on the magnitude of the second mode. Therefore, this mode is absent from the micro-mechanical model. Increasing the coordination number (by adding particles) would bring additional modes that would likewise be unaccounted for in a micro-mechanical model driven by $\overline{D}_{ij}$.

Acknowledgements

This paper resulted from research conducted under the AT22 Research Project Stress Transfer in Granular Media conducted at the U.S. Army Engineer Research and Development Center. Permission was granted by the Chief of Engineers to publish this information.

The author would also like to acknowledge Drs. Antoinette Tordesillas and Bruce Gardiner, and Mr. Stuart Walsh, all from the Department of Mathematics and Physics of the University of Melbourne, for their thoughtful review of this work. Also, the author greatly appreciates Dr. Ernie Heymsfield from the University of Arkansas for the many hours of discussion on fundamental ideas expressed in this paper.

References

1. H.M. Jaeger, S.R. Nager and R.P. Behringer, The physics of granular media. *Physics Today* 49 (1996) 32–38.
2. K.C. Valanis and J.F. Peters, Ill-posedness of the initial and boundary value problems in non-associative plasticity. *ACTA Mech.* 114 (1996) 1–25.
3. P.A. Cundal and O.D.L. Strack, A discrete numerical model for granular assemblies. *Geotechnique* 29 (1979) 47–65.
4. C.S. Chang and C.L. Liao, Constitutive relation for a particulate medium with the effect of particle rotation. *Int. J. Solids Struct.* 26 (1990) 437–453.
5. C.L. Liao, T.C. Chan, A.S.K. Suiker and C.S. Chang, Pressure-dependent elastic moduli of granular assemblies. *Int. J. Num. Anal. Methods Geomech.* 24 (2000) 265–279.
6. R.D. Hryciw, S.A. Raschke, A.M. Ghalib, D.A. Horner and J.F. Peters, Video tracking for experimental validation of discrete element simulations of large discontinuous deformations. *Computers Geotechn*. 21 (1997) 235–253.
7. D.A. Horner, J.F. Peters and A. Carrillo, Large scale discrete element modeling of vehicle-soil interaction. *ASCE J. Eng. Mech.* 127 (1979) 1027–1032.
8. P.A. Cundal, A discrete future for numerical modeling. In: B.K. Cook and R.P. Jensen (eds.), *Discrete Element Methods: Numerical Modeling of Discontinua*. ASCE Geotechnical Special Publication No. 117. Reston (VA): ASCE (2002) pp. 3–4.
9. A. Tordesillas and S. Walsh, Incorporating rolling resistance and contact anisotropy in micromechanical models of granular media. *Powder Technol.* 124 (2002) 106–111.
10. J.P. Bardet and I. Vardoulakis, The asymmetry of stress in granular media. *Int. J. Solids Struct.* 38 (2001) 353–367.
11. B. Bagi, Stress and strain in granular assemblies. *Mech. Materials* 22 (1996) 165–177.
12. B. Bagi, Microstructural stress tensor of granular assemblies with volume forces. *ASME J. Appl. Mech.* 66 (1999) 934–936.
13. N.P. Kruyt, Statics and kinematics of discrete Cosserat-type granular materials. *Int. J. Solids Struct.* 40 (2003) 511–534.
14. J.F. Peters and E. Heymsfield, Application of the 2-D constant strain assumption to FEM elements consisting of an arbitrary number of nodes. *Int. J. Solids Struct.* 40 (2003) 143–159.
15. K.C. Valanis and J.F. Peters, An endochronic plasticity theory with shear-volumetric coupling. *Int. J. Num. and Anal. Methods Geomech.* 15 (1991) 77–102.

16. K.C. Valanis and C.F. Lee, Endochronic plasticity: physical basis and applications. In: C.S. Desai and R.H. Gallagher (eds.), *Mechanics of Engineering Materials*. New York: Wiley (1984) pp. 591–609.
17. D.Z. Zhang and R.M. Raueszahn, Stress relaxation in dense and slow granular flows. *J. Rheology* 45 (1979) 1019–1041.